Hunting the elusive shallow n-type donor – an *ab initio* study of Li and N co-doped diamond

Sergio Conejeros[1,2], M. Zamir Othman[1,3], Alex Croot[1], Judy N. Hart[4], Kane M. O'Donnell[5], Paul W. May[1,*] and Neil L. Allan[1,*]

1. School of Chemistry, University of Bristol, Bristol BS8 1TS, United Kingdom

2. Departamento de Química, Universidad Católica del Norte, Av. Angamos 0610, Antofagasta, Chile, 1240000.

3. Faculty of Science and Technology, Islamic Science University of Malaysia, Nilai, Malaysia

4. School of Materials Science & Engineering, UNSW Sydney, NSW 2052 Australia

5. Department of Physics, Astronomy and Medical Radiation Science, Curtin University, Bentley, WA 6102, Australia

[*] Corresponding authors. Email: Paul.May@bristol.ac.uk (Paul May); N.L.Allan@bristol.ac.uk (Neil Allan)

ABSTRACT

We report calculated energetics (at the GGA, and at the B3LYP, HSE06 hybrid density functional levels of theory) and electronic properties (B3LYP, HSE06) of Li and N co-doped diamond containing LiN_x clusters (x = 1-4). Defect energies and structural properties at the GGA and hybrid (B3LYP, HSE06) levels of theory are very similar. Our results for isolated Li and N dopants agree with previous work in that they are not suitable candidates for shallow n-type donors. Here, we investigate the effects of addition of N atoms as a co-dopant with Li, which vary with the Li:N ratio and whether Li is interstitial or substitutional. Reaction energies, geometries, bonding and densities of states (DOS) are examined. Nitrogen stabilises substitutional rather than interstitial lithium. Atom-projected DOS show that the chief contributions to the defect states are not from orbitals on the dopant atoms themselves but from states associated with neighbouring carbon atoms. Only the tetrahedral 1:4 cluster, Li_CN_4, with substitutional Li is likely to behave as a shallow donor. We propose a non-molecular synthetic route for preparation of the Li_CN_4-doped material via prior generation of the N_4V centre at temperatures at which Li is mobile but Li_CN_4 clusters are not.

Keywords: Semiconductors, diamond, n-type doping, co-dopants, density functional theory

1. Introduction

Due to their increasing availability and affordability from a number of commercial suppliers, chemical vapour deposition (CVD) diamond films are beginning to find a growing number of technological applications [1]. Doping diamond with boron allows p-type semiconducting material to be deposited, with films ranging in conductivity from highly insulating to near metallic [2]. This has enabled the fabrication of many simple p-type devices, such as sensors and electrochemical electrodes [3-5]. But for more complex devices, such as microprocessors, both p-type and n-type behaviour are required. Unfortunately, it has proven extremely difficult to find a dopant for diamond that imparts n-type semiconducting characteristics suitable for use in electronic devices [6].

Nitrogen is one possible dopant [7,8] and nitrogen-doped diamond has been successfully synthesised using various CVD techniques [9,10]. However, the experimental nitrogen energy level in diamond lies 1.7 eV below the conduction band minimum (CBM) [11]. This high excitation energy classifies N as a deep donor, and is therefore useless for most

electronic devices [12]. Alternatively, phosphorus has been used to n-dope CVD diamond films successfully, but the films are not sufficiently conducting for many device applications [13]. Lithium has also been suggested as a possible shallow donor. Kajihara *et al*. concluded that interstitial Li atoms should act as shallow donors in diamond, with an excitation energy of only 0.1 eV required to move an electron from the donor level to the CBM [14]. The large energy associated with incorporating Li leads to theoretical predictions of very low solubility of Li in diamond [14]; this can be overcome to some extent using diffusion techniques in which Li concentrations as high as 10^{19} cm^{-3} have been reported [15]. In addition, under the standard high-temperature conditions used for CVD growth of diamond films, Li has a relatively high mobility [14,16,17], leading to non-uniform concentration profiles, inhomogeneous doping, and formation of Li clusters.

In addition to occupying interstitial sites, Li can also substitute for C or fill a vacancy. It then acts as a deep acceptor, rather than as a shallow donor [18]. Interstitial and substitutional Li can compensate each other, leading to electrical inactivity. This self-compensation led previously to a decline of interest in such an apparently "unpromising" dopant [16,19,20]. The self-compensation would, of course, not occur if only one mode of incorporation could be achieved experimentally, but, unfortunately, this has proven extremely difficult [21].

Recently, in pursuit of the elusive shallow donor for n-type diamond films, attention has again focused on possible incorporation of other elements less commonly used as dopants [22], and interest in Li doping has been rekindled, both as a single Li atom, or together with a second element (co-doping) such as boron [23]. Theoretical studies by Mainwood *et al.* and Goss *et al.* have examined the incorporation of Li [16-18,24-27]. In particular, the effects of clustering which inhibits the ability of Li atoms to perform as shallow donors have been investigated [16]. These studies also concluded that the lowest-energy interstitial position is a tetrahedral site, and that incorporation of Li at a pre-existing vacancy site is preferred to interstitial incorporation by at least 1.7 eV [16,18,24,25].

Li can also play an interesting role at the diamond surface. Lithiation, *i.e*. addition of LiO groups to the diamond surface, has been shown both experimentally [28] and theoretically [29,30], to induce negative electron affinity (NEA), as does hydrogenation. Moreover, such lithiated surfaces remain stable at temperatures up to 1000 K. These NEA surfaces enhance the emission of electrons from the bulk diamond into the vacuum

[28,30,31], which is a key requirement for field emission devices and thermionic energy converters. Other groups have used DFT to explore the effects of a variety of surface-terminating species, such as MgO, which has also recently been studied experimentally [32], F, Cl, Br, CoO, CuO, and TiO [29,33-37]. Even so, many applications of NEA diamond, particularly thermionic emission, still require n-type doping of the bulk, making identification of potential shallow-donor dopants particularly important [38-41].

Co-doping is a potential way forward. Possible combinations include B-N [42,43], B-P [44] and Li-N. Experimental incorporation of both Li and N in CVD diamond films has been reported [45,46]. High concentrations of Li (~10^{19} cm^{-3}) and N (~10^{21} cm^{-3}) were achieved simultaneously, but with no control of the mode of incorporation. No correlation was found between the Li/N content and the film conductivity, and the films remained electrically inactive.

In this paper, results of both density functional theory (DFT using the generalised gradient approximation, GGA) and hybrid density functional theory (B3LYP and HSE06) calculations are reported to obtain a better understanding of the behaviour – both thermodynamic and electronic – of Li and N in diamond in order to guide new experimental work. While GGA, the simpler DFT implementation, gives good values for the defect thermodynamics in agreement with the hybrid methods, it includes a poorer representation of the exchange interaction, plus the band gap is severely underestimated, which is precisely the location of the defect states. We consider in detail the results of co-doping with Li and N and identify shallow donor atom clusters Li_CN_x (<0.2 eV) that could be formed in the diamond lattice. A Li_CN_4 complex comprising a substitutional Li and four adjacent N atoms has been suggested by Moussa *et al.* as a shallow donor on the basis of calculated activation energies [47], but these authors did not carry out hybrid calculations, consider interstitial Li, examine the thermodynamics and bonding in detail, present the density of states or consider other arrangements of the nitrogen atoms. We examine the electronic structure and energetics of this and other complexes in detail, and also propose a preparative route to the most promising complex, which should aid future experimental doping studies and realisation of n-type diamond.

2. Theoretical/computational methods

Periodic DFT calculations on doped diamond used a 64-atom (cubic) supercell constructed from a 2×2×2 expansion of the cubic diamond unit cell. To assess any supercell size effects and check convergence with cell size, some calculations were repeated with 144-atom (tetragonal), 216-atom (cubic) and 512-atom (cubic) supercells. Details are in the Supplementary Information. For each functional tested, we first generated fully optimised (lattice parameter and basis atom positions) structures for bulk intrinsic diamond. We subsequently optimised supercells of Li-doped, N-doped and Li-N co-doped diamond. For substitutional dopants, carbon atoms in the supercell were directly replaced by the dopant of interest (Li or N). We label a substitutional Li as Li_C. Interstitial lithium, which we label with an additional subscript $Li_{i,}$ were placed at the T_d (tetrahedral site), consistent with previous work [16,24,25,48]. To examine co-doping, between 1 and 4 of the nearest-neighbour carbon atoms surrounding the Li atom were replaced by N, as illustrated in Fig. 1 for Li_CN_4.

The energies of the doped supercells were minimised with respect to the positions of the atoms only. Optimisations with fixed unit-cell dimensions strictly give internal energy changes at constant volume. Nevertheless, such defect energies serve also as an excellent approximation for defect enthalpies at constant pressure [49]. Here, calculations relaxing all degrees of freedom gave almost identical results to those in which the supercell lattice parameters were fixed. No symmetry constraints were applied in any of the supercell optimisations. Where relevant, energies of the different possible spin states were calculated. We shall see that these different spin states generally have the same energy to within a few meV.

First, periodic (DFT) calculations were carried out using the plane-wave code CASTEP [50,51], with a planewave valence basis set of energy up to 800 eV, and ultra-soft core electron pseudopotentials. The generalised gradient approximation (GGA) with the Perdew-Burke-Ernzerhof (PBE) exchange-correlation functional was used [52]. The Monkhorst-Pack grid for *k*-point sampling of the Brillouin zone was set at 4×4×4; convergence with respect to the number of *k*-points was checked. During optimisation, the geometries were deemed to be converged when the total forces on all the atoms were < 0.005 eV/Å. The OptaDOS utility [53] was used to plot the densities of states (DOS).

Second, we used the *ab initio* periodic code CRYSTAL17, on grounds of computational cost, for hybrid density-functional-theory–Hartree-Fock calculations (B3LYP, HSE06)

[54,55]. A number of doped-diamond supercell calculations using the CRYSTAL program have been reported previously [42,43,56-64]. This code uses localised Gaussian basis sets to evaluate energies and associated electronic properties [65-67]. The basis sets used were 6-21(d-G) for C [68] and pob-TZVP for Li and N [69]. For the calculation of the Coulomb and exchange integrals, tolerance factors of 7, 7, 7, 7, and 14 were used [67]. The convergence criterion for the energy was 10^{-7} au and the *k*-point sampling 4×4×4 [70] and satisfactory convergence with respect to these parameters is demonstrated explicitly in the Supplementary Information.

All the defects and defect clusters considered in this paper are neutral (*i.e*. uncharged). The formation energies of the defects, ΔE_{f}, are calculated [71] using:

$$\Delta E_{\mathrm{f}} = E_{\mathrm{tot}}^{\mathrm{Def}} - E_{\mathrm{tot}}^{\mathrm{In}} - \sum n_i \mu_i \qquad (1)$$

where $E_{\mathrm{tot}}^{\mathrm{Def}}$ is the energy of the doped (defective) diamond supercell, $E_{\mathrm{tot}}^{\mathrm{In}}$ is the energy of the undoped (intrinsic) diamond supercell of the same size, *n* the number of atoms added to (+) or removed from (–) the supercell, and μ_i the chemical potential of the atom *i* added or removed. The chemical potential for a Li atom was determined from a calculation of bulk Li metal, so that all our chemical reactions relate to incorporation of Li from Li metal. Experimentally, solid Li_3N [46] or gaseous organo-lithium precursors [72] are often used as the source of Li, and it may well be that it is free Li atoms created in the aggressive hot CVD environment which enter the diamond; we comment later on the consequences for our calculated values of ΔE_{f}. For N, we have chosen as reference an isolated N atom rather than molecular N_2 because it is the more relevant species in the growth process in the CVD reactor [73,74]. The C chemical potential was taken from the calculations on pure diamond. All terms in Equation 1 were calculated at the same level of theory.

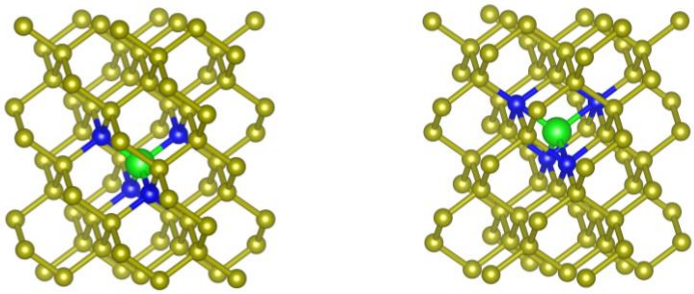

Fig 1. Two LiN_4 clusters studied: (a) substitutional Li (Li_CN_4) and (b) interstitial (Li_iN_4) with the interstitial atom at the T_d site. C atoms are yellow, N atoms are blue and Li atoms are green.

3. Results and discussion

3.1 Bulk Diamond

For validation purposes, we start with the structure and properties of bulk (undoped) diamond. The calculated GGA, B3LYP and HSE06 optimised unit cell parameters are 3.568 Å, 3.594 Å and 3.571 Å, respectively, all in good agreement with experiment (3.567 Å) [75,76]. The corresponding C-C bond length is 1.55 Å (experiment 1.54 Å).

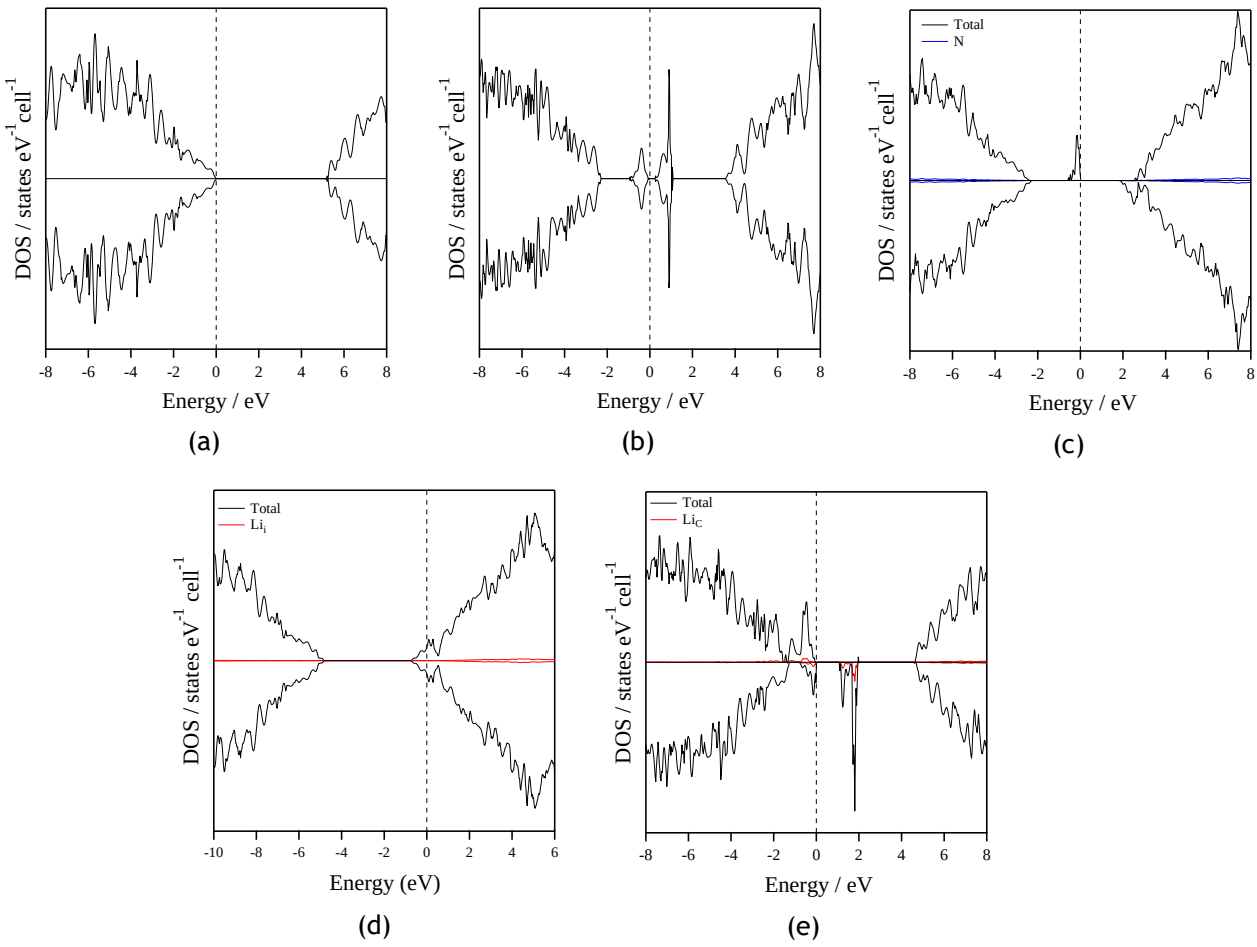

Fig. 2. Hybrid (HSE06) DOS of (a) pure diamond, (b) carbon vacancy and (c) N-doped diamond (S = ½) with substitutional nitrogen for the 64-atom supercell. (d) Hybrid (HSE06) DOS of Li_i-doped diamond (interstitial, T_d site) for the 65-atom supercell (S = ½). (e) Hybrid (HSE06) DOS of Li-doped diamond (substitutional) from the 64-atom supercell. In (c), (d), (e) and (f) both the total DOS and the projected DOS for the dopant atom are shown. In this and all subsequent figures, the energy of the highest occupied state is arbitrarily set to zero and indicated by the vertical dashed lines. The upper and lower frames show the DOS for spin-up and spin-down electrons, respectively.

The GGA calculated band gap is 4.06 eV, in agreement with the value (~4.1 eV) calculated using similar methods by Lombardi *et al*. [24] This is significantly lower than the experimental value of 5.45 eV [76], a well-known discrepancy due to the limitations of DFT in its treatment of exchange and correlation, as mentioned in the introduction. Hybrid functionals that incorporate a proportion of exact exchange give more accurate electronic

properties and, while accurate calculation of band gaps remains challenging [77,78], such methods offer many advantages over GGA [79]. The variation in band gap from one system to another should also be reliable with hybrid methods.

Fig. 2a shows the density of states (DOS) of pure diamond calculated with HSE06; the band gap calculated with HSE06 is 5.19 eV, which is in much better agreement with the experimental value (5.45 eV) than the GGA result. For comparison, the B3LYP band gap is 5.72 eV. For reasons of space, we present only HSE06 DOS in this paper since the conclusions from the similar B3LYP DOS are the same.

3.2 Nitrogen in Diamond

The energy, ΔE_f, of substitution of a C atom in the 64-atom supercell by N, where the initial state of N is the atomic gas (Equation (2) in Table 1), is -0.8 eV per N incorporated (GGA), -1.1 eV (B3LYP) and -1.3 eV (HSE06), indicating that the reaction is energetically favourable. Note that if the reactant is the nitrogen molecule N_2 rather than the N atom, as would be appropriate for ambient, rather than CVD reactor, conditions, all energies involving nitrogen in Table 1 increase by ~4.9 eV, making direct incorporation of nitrogen into undefective diamond extremely unfavourable. We repeated the B3LYP calculation for a diamond supercell containing 144 atoms and the value remained unchanged to two significant figures, confirming convergence with supercell size; further tests of convergence with system size are given in the Supplementary Information.

There is considerable symmetry breaking in the optimised structures, regardless of method. The symmetry at the nitrogen site is reduced to C_{3v}. The three nearest-neighbour C-N bonds in the optimised HSE06 structure are 1.47 Å, which is 0.08 Å shorter than the C-C bonds in diamond, while the fourth is much longer, 2.03 Å, reflecting repulsion between the lone pair on nitrogen and the unpaired electron in the "dangling" bond. Changes in the surrounding C(nearest-neighbour) - C(next-nearest-neighbour) distances are small, approximately ±1.0%. The lengths of C-C bonds situated further away from the dopant atom are found to remain unchanged, showing that the structure is strained only very locally within a few atoms of the dopant position. Our calculated geometry is in very good agreement with previous work [60].

If there is a pre-existing vacancy in the diamond structure that is subsequently occupied by N (Equation (3) in Table 1), the formation energy is reduced dramatically to -7.5 eV (GGA), -8.4 eV (B3LYP) or -9.3 eV (HSE06). These negative formation energies suggest that addition of N atoms into the diamond structure depends mainly on the availability of vacancy sites [80,81]. Such vacancies arise as a direct result of the CVD growth process, which typically takes place at 1100 K, and have been observed both experimentally [82,83], at concentrations up to 50 ppm [84], and in computer simulations of diamond growth [85-87].

The hybrid (HSE06) DOS in Fig. 2c for the nitrogen-doped supercell shows a deep donor level in the centre of the band gap consistent with experiment [6] and also a minority-spin acceptor level, approximately 4.2 eV above the valence band maximum (VBM). Similar features have been noted by Ferrari *et al*. [60] in B3LYP calculations. In agreement with these authors, we too see, interestingly, that the majority of both the donor-band and the acceptor-band states arise not from states on *nitrogen* but on the nearest-neighbour *carbon* atom at 2.03 Å with the unpaired electron in the dangling bond. The Mulliken charges are -0.33*e* on N, +0.17*e* on the three C neighbours at 1.47 Å and +0.05*e* on the C at 2.03 Å and are negligible on all atoms further from the nitrogen. The bond populations between N and the three equivalent carbon neighbours are +0.27*e*; in contrast between N and the fourth C the bond population is -0.09*e* indicating an antibonding interaction. The spin density is largest on the carbon at 2.03 Å (+0.76*e*); on the N itself it is only +0.17*e*.

Table 1. Chemical equations and calculated GGA, B3LYP and HSE06 energies for incorporation of single dopants in diamond. Energies are given in eV per Li or N atom incorporated. V_C denotes a carbon vacancy while Li and Li_i denote substitutional and interstitial Li, respectively. Reference states of nitrogen and lithium are the gaseous N atom, and solid Li, respectively.

	GGA	B3LYP	HSE06	
Nitrogen-doped diamond				
From intrinsic diamond:				
$C_{64}(s) + N(g) \rightarrow C_{63}N(s) + C(s)$	-0.8	-1.1	-1.3	(2)
$C_{144}(s) + N(g) \rightarrow C_{143}N(s) + C(s)$		-1.1		
From pre-existing vacancy				
$C_{63}V_C(s) + N(g) \rightarrow C_{63}N(s)$	-7.5	-8.4	-9.3	(3)
$C_{143}V_C(s) + N(g) \rightarrow C_{143}N(s)$		-8.4		
Li-doped diamond (interstitial Li, Li_i)				
From intrinsic diamond:				
$C_{64}(s) + Li(s) \rightarrow C_{64}Li_i(s)$	8.4	9.1	9.5	(4)
$C_{144}(s) + Li(s) \rightarrow C_{144}Li_i(s)$		9.1		
Li-doped diamond (substitutional Li)				
From intrinsic diamond:				
$C_{64}(s) + Li(s) \rightarrow C_{63}Li(s) + C(s)$	8.3	8.6	9.1	(5)
$C_{144}(s) + Li(s) \rightarrow C_{143}Li(s) + C(s)$		8.4		
From pre-existing vacancy				
$C_{63}V_C(s) + Li(s) \rightarrow C_{63}Li(s)$	1.6	0.8	1.1	(6)
$C_{143}V_C(s) + Li(s) \rightarrow C_{143}Li(s)$		0.7		

3.3 Lithium in Diamond

3.3.1 Interstitial Li, Li_i

Previous work has suggested that the T_d site is the most favourable for interstitial Li, and so we have used this site in this work [16,24,25,48]. Our solution is metallic, with Li_i-C bond lengths of 1.63 Å, 1.63 Å, 1.67 Å (2×) (HSE06), thus reducing the tetrahedral symmetry to C_{2v}. There is substantial variation in some of the C(nearest-neighbour) - C(next-nearest-neighbour) bond lengths which vary from 1.49 Å to 1.94 Å. Overall, this suggests that the diamond lattice is significantly strained by the introduction of interstitial lithium, more so than for nitrogen doping, and consistent with the higher formation energies.

Fig. 2d shows the HSE06 DOS. The dopant band, largely comprising states from one of the neighbouring carbons at 1.63 Å and one of the next-nearest carbons at 1.81 Å, merges with the conduction band, giving rise to the Fermi level lying within and close to the bottom of the conduction band. Experimentally realistic, lower Li concentrations, require a larger supercell than we are able to study; these could well be non-metallic and consistent with shallow-donor activity.

3.3.2. Substitutional Li, Li_C

When Li is substitutional, the tetrahedral symmetry at the site is lost and the symmetry becomes C_s; the four nearest-neighbour carbons lie at distances from Li of 1.762 Å, 1.769 Å, 1.769 Å and 1.784 Å (HSE06); these are all~0.1 Å larger than those for Li_i-C. Accompanying this increase is a decrease in the surrounding C(nearest-neighbour) - C(next-nearest-neighbour) distances by around 4.0%. The lengths of C-C bonds situated further away from the dopant atom are found to remain largely unchanged.

The HSE06 DOS for lithium-doped diamond with substitutional Li (Fig. 2e) is markedly different from that for interstitial Li (Fig. 2d). Removal of a carbon from the unit cell creates four dangling bonds, one on each of the neighbouring C atoms. Insertion of a Li atom at this site supplies one electron and formally removes one dangling bond. The new states which appear at the top of the valence band in the doped system arise from the four nearest-neighbour carbon atoms, with only a small contribution from Li. There are three unpaired electrons – the lowest energy spin state is $S = 3/2$ which is only ≈15 meV lower in

energy than S = ½. The unoccupied spin-down peaks form an acceptor band 1-2 eV above the valence band; the states in this band all also come from the four nearest-neighbour carbons, with only approximately 5% from the Li. Thus, this structure produces neither an acceptor nor a donor, in agreement with previous work [18,24,25]. We note that as with the substitutional nitrogen defect, while the new levels in the band gap *arise* from the presence of nitrogen or lithium, the levels are not, *per se*, N or Li levels.

The Mulliken charges are all very small: +0.08e on Li, -0.06e on the four nearest carbon neighbours, and very small but positive (+0.01e) on the next-nearest carbon neighbours. The spin densities vary rather more on the four nearest-neighbour carbons, decreasing with distance in the order +0.63e, +0.61e, +0.61e and +0.54e. On the Li itself, the spin density is +0.25e. Li-C Bond populations are +0.144e, +0.152e, +0.152e and +0.174 increasing with increasing bond length.

3.3.3 Thermodynamics of Li incorporation

GGA energies, ΔE_f, for interstitial and substitutional incorporation of Li (Equations (4) and (5), respectively, in Table 1) taking solid Li as the initial Li state are 8.4 eV and 8.3 eV per Li, respectively; the corresponding HSE06 hybrid energies are slightly higher at 9.5 and 9.1 eV, while B3LYP gives intermediate values. Taking gaseous Li as the initial Li state, these energies are reduced by 1.6 eV.

The Li-C bonds in molecular compounds such as methyl lithium (2.31 Å) [88] and phenyl lithium (2.24–2.33 Å) are much longer than those found in Li-doped diamond (at both interstitial and substitutional sites) [89], suggesting that the Li-C bonds in diamond are greatly compressed and the resulting strain contributes to high positive energies of Li incorporation in the absence of pre-existing vacancies.

If the Li dopant occupies an existing vacancy site (Equation (6) in Table 1), the formation energy is significantly reduced to only 1.6 eV (GGA), 0.8 eV (B3LYP) and 1.1 eV (HSE06) taking solid Li as the initial Li state. With the reference state of Li taken as the gaseous atom, the energy of incorporation is again further reduced by 1.6 eV per Li atom, reducing this energy to near-zero or negative values. The formation energy is much lower for this process than incorporation of Li where there is no pre-existing vacancy, and so Li introduced during diamond growth will predominantly occupy such vacancy sites [18].

Unless such vacancy sites are present, or are generated during synthesis, only a small amount of Li is likely to be incorporated, and any introduced Li will occupy both interstitial and substitutional sites, due to their similar formation energies.

3.4 Li-N Co-doped Diamond

The combination of N deep-donor properties and Li shallow-donor properties through introduction of a Li_CN_4 complex in diamond has been predicted to promote shallow donor properties on the basis of calculation of donor and acceptor activation energies [47]. However, there has previously been no systematic study of LiN_x defects for different x, no hybrid DFT level calculations, and no investigation of the energetics of dopant incorporation. Thus, we turn to diamond co-doped with Li (interstitial and substitutional) and N, Li_iN_x and Li_CN_x (x = 1-4), and discuss the synthetic implications. Table 2 lists the calculated formation energies for the formation of LiN_x defects, with both substitutional and interstitial Li.

We first consider LiN. The energy of formation of Li_iN co-doped diamond from intrinsic diamond, with Li at the T_d interstitial site adjacent to the nitrogen (Table 2, Equation (7)), is high (5.0 eV for HSE06), and the energy for the incorporation of interstitial Li into diamond already N-doped even higher (Table 2, Equation (8)). However, the formation energy values are lower than for the Li-doped diamond, suggesting that the strain introduced by the long Li-C bonds is reduced by the presence of nitrogen. The energy of insertion of Li and N atoms into adjacent *substitutional* sites forming Li_CN is ≈ 2 eV (Equation (9), Table 2), over 2 eV lower than for interstitial Li. The formation energy values for co-doping are again lower than those for Li-doped diamond. Thus, the presence of N favours the incorporation of Li into diamond, and strongly favours substitutional rather than interstitial Li, in contrast to Li incorporation in intrinsic diamond where there is little difference between the formation energies of substitutional and interstitial Li (Equations (4) and (5), Table 1). For N-doped diamond containing a vacancy adjacent to the nitrogen, the formation energy for Li_CN co-doped diamond reduces even further to ~1 eV (Equation (11), Table 2). Thus, all the different methods indicate that, while still endothermic, Li_CN co-doped diamond is formed more readily than Li-doped diamond.

Increasing the number of nitrogen atoms in the cluster leads to a successive overall lowering of formation energies and increased favouring of substitutional over interstitial Li

(Table 2). Even for Li_CN_2, the formation energy from intrinsic diamond is exothermic (Equation (13), Table 2). Even though the formation energies of Li_CN_3 and Li_CN_4 are so much more negative than that of Li_iN_3 and Li_iN_4, respectively, the formation energies of the latter are, nevertheless, negative and they could possibly be kinetically stable.

The Supplementary Information contains a detailed survey of the spin states, geometries and electronic structures of Li_iN_x (x = 1-3) and Li_CN_x (x = 1-3). None of these give rise to a shallow donor band. We now turn to consider in detail the suggested cluster of Moussa *et al*. [47], Li_CN_4, and briefly other clusters involving Li and four nitrogens.

Table 2. Chemical equations and calculated GGA, B3LYP and HSE06 energies for the formation of Li_iN_x and Li_CN_x defects in a 64-atom diamond supercell. Energies are in eV per Li atom incorporated. NV denotes nitrogen-doped diamond, with a vacancy V_C adjacent to the nitrogen. Reference states of nitrogen and lithium are the gaseous N atom, and solid Li, respectively.

	GGA	B3LYP	HSE06	
LiN				
Interstitial Li, from intrinsic diamond: $C_{64}(s) + Li(s) + N(g) \rightarrow C_{63}LiN(s) + C(s)$	4.5	4.9	5.0	(7)
Interstitial Li, from N-doped diamond: $C_{63}N(s) + Li(s) \rightarrow C_{63}LiN(s)$	5.3	5.9	6.2	(8)
Substitutional Li, from intrinsic diamond: $C_{64}(s) + Li(s) + N(g) \rightarrow C_{62}LiN(s) + 2C(s)$	1.8	2.0	3.1	(9)
Substitutional Li, from N-doped diamond: $C_{63}N(s) + Li(s) \rightarrow C_{62}LiN(s) + C(s)$	2.6	3.0	4.3	(10)
Substitutional Li, from NV in diamond: $C_{62}NV_C(s) + Li(s) \rightarrow C_{62}LiN(s)$	1.2	0.9	2.0	(11)
LiN_2				
Interstitial Li, from intrinsic diamond: $C_{64}(s) + Li(s) + 2N(g) \rightarrow C_{62}LiN_2(s) + 2C(s)$	2.4	2.7	2.6	(12)
Substitutional Li, from intrinsic diamond: $C_{64}(s) + Li(s) + 2N(g) \rightarrow C_{61}LiN_2(s) + 3C(s)$	-4.6	-4.4	-4.5	(13)
LiN_3 defect				
Interstitial Li, from intrinsic diamond: $C_{64}(s) + Li(s) + 3N(g) \rightarrow C_{61}LiN_3(s) + 3C(s)$	-1.0	0.2	-0.1	(14)
Substitutional Li, from intrinsic diamond: $C_{64}(s) + Li(s) + 3N(g) \rightarrow C_{60}LiN_3(s) + 4C(s)$	-10.8	-10.7	-11.1	(15)
LiN_4 defect				
Interstitial Li, from intrinsic diamond: $C_{64}(s) + Li(s) + 4N(g) \rightarrow C_{60}LiN_4(s) + 4C(s)$	-2.6	-1.3	-2.6	(16)
Substitutional Li, from intrinsic diamond: $C_{64}(s) + Li(s) + 4N(g) \rightarrow C_{59}LiN_4(s) + 5C(s)$	-14.7	-13.6	-14.5	(17)

3.4.1 Li_iN_4 and Li_CN_4

The relative stabilities of Li_iN_4 and Li_CN_4 are reflected in their geometries. Li_iN_4 is extremely distorted (supplementary information) and the corresponding DOS shown in Fig. 4a, with its mid-gap defect states, shows that this cluster does not generate shallow donor states.

In contrast, Li_CN_4 is tetrahedral and local C_{3v} symmetry is preserved at the nitrogens in Li_CN_4. Figure 3 collects together the calculated bond lengths, Mulliken charges and bond populations. All Li-N bonds are 1.72 Å, an increase of 0.08 Å from that in Li_CN, while all N-C bonds are 1.49 Å, 0.02 Å larger than in the system doped with nitrogen alone. The next-nearest-neighbour carbon atoms from the nitrogen are all ~1.55 Å from the nearest-neighbour carbons, showing that the perturbation of the lattice is very local and decays rapidly.

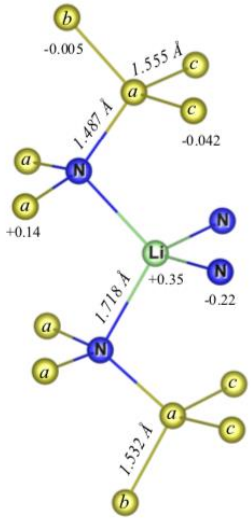

Fig. 3. Bond lengths (in italics) and Mulliken net charges (in *e*) in Li_CN_4. The labels *a*, *b* and *c* denote symmetrically equivalent carbon atoms.

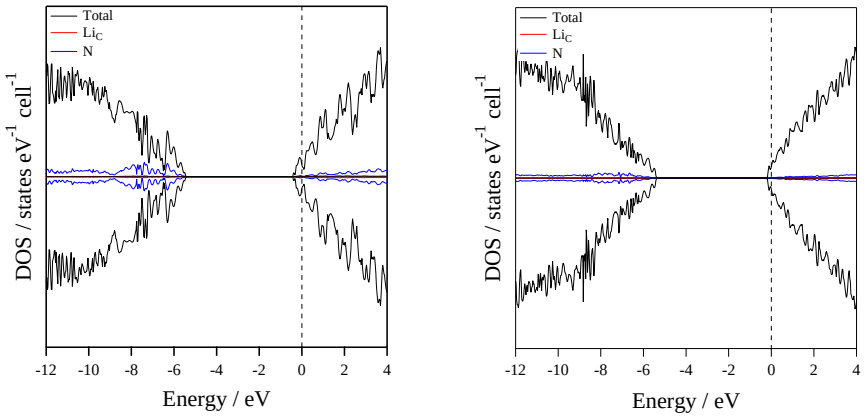

Fig. 4. (a) and (b): Hybrid (HSE06) DOS for Li_CN_4 co-doped diamond (substitutional) for (a) 64- and (b) 144-atom supercells, $C_{59}Li_CN_4$.and $C_{143}Li_CN_4$, respectively. The total DOS and the projected DOS for the dopant atoms are shown. The highest occupied states are arbitrarily assigned a value of zero and are indicated by vertical dashed lines. Note these are diamagnetic conducting solutions.

Calculated Mulliken charges are: +0.35*e* on Li, -0.25*e* on each of the four nearest nitrogen neighbours, and positive (+0.14*e*) on the carbons bonded to N. Bond populations are +0.074*e* for Li-N, reflecting the ionic nature of the bond, +0.231*e* for N-C, close to +0.27*e* for that in the purely N-doped system and +0.377*e* for the (nearest-neighbour)C - (next-nearest-neighbour)C, this last value reflecting the shorter bond length compared to that in pure diamond.

The DOS of Li_CN_4 is shown in Fig. 4. At the very high dopant concentrations in the range imposed by the supercell calculations, one might expect shallow donor levels to merge with the conduction band, with a diamagnetic solution lower in energy. This is indeed so for both the 64-atom and 144-atom supercells shown in this figure. It is interesting to note that these levels are not associated with orbitals on the Li or N atoms but from the carbons directly bonded to the Li_CN_4 cluster. With larger supercells of 216 atoms and 512 atoms, these occupied states start to separate off from the conduction band. Corresponding band structures are given in the Supplementary Information.

We have also estimated a Li_CN_4 donor activation energy of 0.37 eV using a 512-atom supercell, using the empirical marker method [27,90,91] with the known P-donor activation

energy of 0.6 eV. Overall, our results suggest that at lower, more experimentally relevant concentrations, Li_CN_4 is a shallow donor with an activation energy of 0.2-0.4 eV. This is consistent with the arguments of Moussa *et al*. [47]. Once again, the vast majority of the new states concerned do not involve states on Li or N; they originate from states on the *carbons* bonded to the nitrogen atoms.

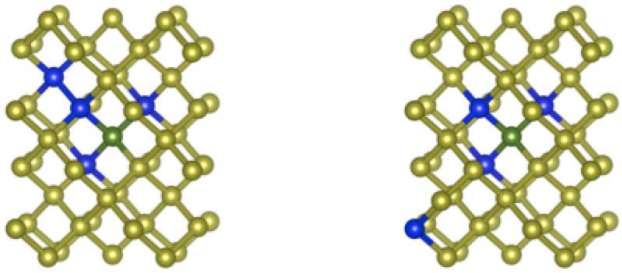

Fig. 5. Unrelaxed geometries of two further possible arrangements of Li_CN_4 clusters (Cluster 2 and Cluster 3). Cluster 1 is shown in Figure 1(a). C atoms are yellow, N atoms blue and Li green.

We have examined two different geometrical arrangements of the Li_CN_4 cluster in which one of the nitrogen atoms is further away from the central Li. In the initial structures, this nitrogen atom occupied a next-nearest neighbour site (which we label as Cluster 2) or a next-next-neighbour site (Cluster 3). The optimised geometries of the two clusters are shown in the Supplementary Information. There is substantial relaxation, particularly in Cluster 2, where an initial N-N distance of 1.55 Å increases to 1.9 Å. These are both considerably higher in energy than the tetrahedral cluster: 1.14 eV (Cluster 2) and 1.75 eV (Cluster 3), respectively – so under thermodynamic control the tetrahedral cluster will dominate. The DOS for Clusters 2 and 3 (also given in the Supplementary Information), are very different from that in Fig. 4(b), with no shallow dopant levels. The DOS for Cluster 2 is broadly similar to that expected for a combination of LiN_3 and LiN (see Supplementary Information), and that for Cluster 3 to a combination of LiN_3 and N.

3.4.2 Stability of Li_CN_x Clusters

Table 3 includes energies for dissociation of Li_CN_x into separate Li_sN_{x-1} and N defects for the 64-atom supercell. All these energies are large and positive, consistent with the decrease in formation energies with increasing N content. For Li_CN_4 (Equation (22), Table 3) we have also examined dissociation to separate Li and four tetrahedrally arranged N atoms (N_4), a reaction which is also extremely endothermic.

Although a single Li_CN_4 defect is thermodynamically stable with respect to isolated N and Li_CN_3 defects by 2-3 eV (Equation (21), Table 3), combining reactions (13), (15) and (17) shows that the reaction between Li_CN_4 and Li_CN_2 to form two Li_CN_3 clusters is exothermic by ≈2 eV. Thus, in principle, Li_CN_4 clusters will be only kinetically stable but this is unlikely to be a problem in practice because of the large dissociation energy of Li_CN_4, Equation (21), and its consequent low mobility.

Table 3. Chemical equations and corresponding GGA, B3LYP and HSE06 energies for the dissociation of Li_CN_x clusters in a 64-atom diamond supercell. Energies are in eV.

	GGA	B3LYP	HSE06	
Li_CN				
$C_{62}LiN(s) + C_{64}(s) \rightarrow C_{63}Li(s) + C_{63}N(s)$	5.8	5.6	4.8	(18)
Li_CN_2				
$C_{61}LiN_2(s) + C_{64}(s) \rightarrow C_{62}LiN(s) + C_{63}N(s)$	5.6	5.4	6.3	(19)
Li_CN_3				
$C_{60}LiN_3(s) + C_{64}(s) \rightarrow C_{61}LiN_2(s) + C_{63}N(s)$	5.4	5.2	5.3	(20)
Li_CN_4				
$C_{59}LiN_4(s) + C_{64}(s) \rightarrow C_{60}LiN_3(s) + C_{63}N(s)$	3.1	1.8	2.2	(21)
$C_{59}LiN_4(s) + C_{64}(s) \rightarrow C_{60}N_4(s) + C_{63}Li(s)$	16.1	17.6	18.1	(22)

3.4.3 Lithium-Rich Clusters

Lithium-rich clusters (Li_yN, y = 2-4) were also investigated, in which all dopants were positioned at substitutional sites, with a central N atom surrounded by y nearest-neighbour Li atoms. The formation energies for all three such Li_yN clusters from pure diamond are extremely high (>10 eV). Thus, a lithium-rich cluster configuration is unlikely to be achieved using known techniques.

3.5 Implications for experimental design

Of the clusters we have examined, our calculations suggest, like those of Moussa *et al*. [47], that Li_CN_4 clusters are the most promising as shallow donors. In this section we consider the thermodynamics of their formation in more detail.

The overall formation of Li_CN_4-doped diamond (with substitutional Li) from diamond containing a vacancy ($C_{63}V_C$) is strongly exothermic:

$$C_{63}V_C(s) + Li(s) + 4N(g) \rightarrow C_{59}LiN_4(s) + 4C(s) \qquad \Delta E_{(B3YLP)} = -21.3 \text{ eV} \qquad (23)$$

Based on this, Fig. 6 shows a possible pathway for the formation of Li_CN_4 defects via the N_4V defect. The vacancy formation energy in diamond – the energy to remove one carbon atom – is high, ≈ 8 eV for a single vacancy, in agreement with previous work [92,93]. Nevertheless, formation of such vacancies is inevitable during the diamond CVD growth process [82-84]. The energies of formation of N_2V, N_3V and N_4V from a pre-existing vacancy (*i.e*. here $C_{63}V$) and N atoms are all exothermic (Fig. 6).

The B3LYP energies in Fig. 6 show that clusters $C_{63-x}N_xV_C$ for x = 2,3,4 but not x = 1 are thermodynamically stable with respect to elimination of the vacancy:

$$C_{63-x}N_xV_C(s) + (x - 1)C_{64}(s) + C(s) \rightarrow xC_{63}N(s) \qquad \begin{array}{l} x = 1,\ \Delta E = \text{ -1.1eV} \\ x = 2,\ \Delta E = \text{ 2.3 eV} \\ x = 3,\ \Delta E = \text{ 7.3 eV} \\ x = 4,\ \Delta E = \text{ 12.1 eV} \end{array} \qquad (24)$$

Figure 6 thus shows that under thermodynamic control, N_2V, N_3V and N_4V centres will all be present, with a lower concentration of NV [94,95]. Consistent with our

thermodynamic analysis is the common occurrence of N_3V and N_4V clusters in natural diamond and also in synthetic high-pressure high-temperature diamond, where they are known as N3 centres and B centres, respectively [96-99]. Thus, as well as CVD, high-pressure heat treatment of single-substitutional N-doped diamond may provide an alternative route to forming N_2V, N_3V and N_4V clusters [100]. Indeed, a huge amount of work has been performed, using techniques such as irradiation of the diamond by high-power electrons or laser light, or implantation of N ions, to increase the concentration of vacancies in N-doped diamond in order to produce the N_xV centres that are proposed for many single-photon quantum applications [101].

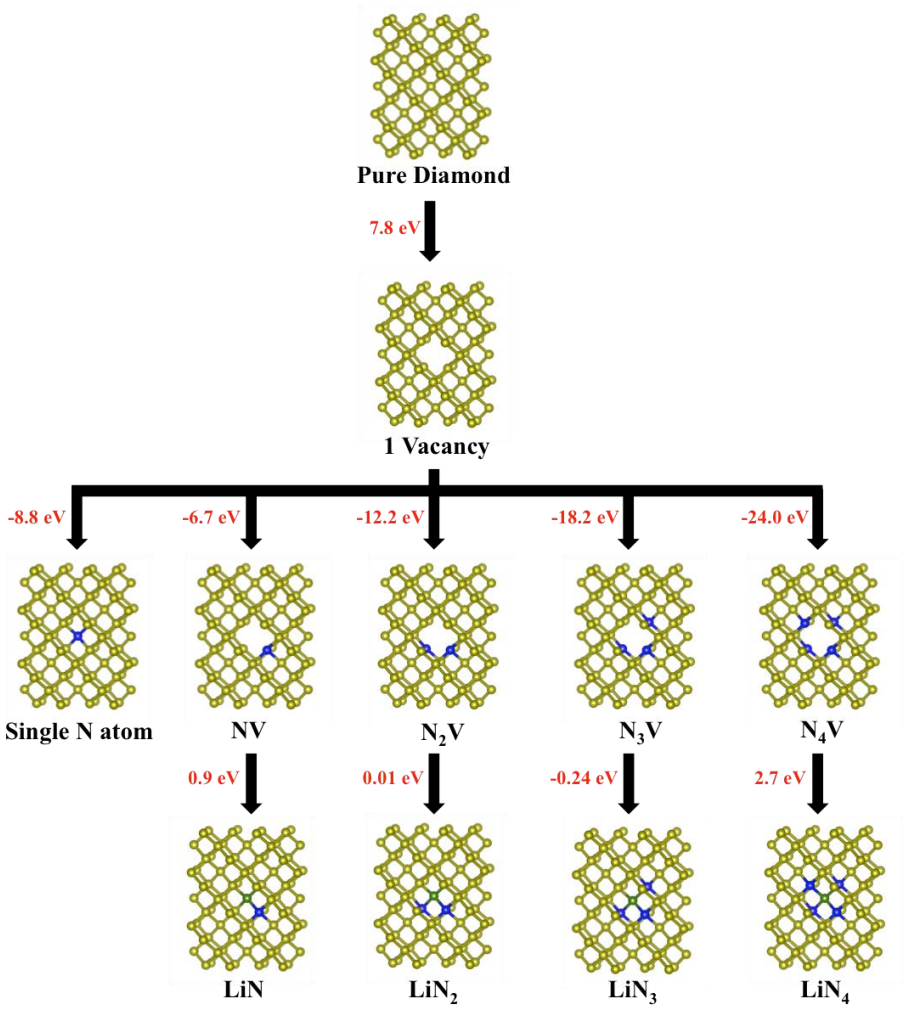

Fig. 6. B3LYP energies of possible experimental pathways for the synthesis of Li_CN_x co-doped diamond. C atoms are yellow, N atoms are blue and Li atoms are green.

The final step in the pathway is to trap a Li atom at the vacancy site in N_4V under thermodynamic control. Starting from lithium *metal*, this is an endothermic process by 2-3 eV. However, starting from Li *atoms* reduces this energy by 1.5 eV, making the process achievable. Furthermore, if pre-existing substitutional and interstitial Li defects in diamond are mobile, the energy of the defect reactions:

$$C_{59}N_4V + C_{63}Li + C \rightarrow C_{64} + C_{59}LiN_4 \qquad \Delta E = -5.9 \text{ eV} \quad (25)$$

$$C_{59}N_4V + C_{64}Li_i \rightarrow C_{64}(s) + C_{59}LiN_4 \qquad \Delta E = -6.2 \text{ eV} \quad (26)$$

are both highly exothermic.

The calculated energies indicate that temperature control is important to ensure that Li atoms are mobile, while isolated vacancies and the Li_CN_4 clusters remain immobile, since, for example, the energy of the reaction:

$$2C_{59}N_4Li + C_{63}V \rightarrow C_{57}LiVN_5 + C_{60}LiN_3 + C_{64} \quad \Delta E = -3.4 \text{ eV} \quad (27)$$

is exothermic by -3.4 eV. There is also the possibility of Li_CN_4 clusters forming larger aggregates that are not shallow donors. While other possible routes involving molecular precursors containing LiN_4 groups have been considered by Moussa *et al.* [47], such precursors and these groups will be rapidly broken down under CVD conditions.

We thus have a potential window-of-opportunity to prepare Li_CN_4 if N_4V is present in sufficiently high concentration. Direct incorporation of Li into diamond has been demonstrated in our previous experimental reports [45,46] but this has yet to be performed using diamond already containing high concentrations of N_4V clusters.

4. Conclusions

We have shown that thermodynamic properties of Li-N co-doped diamond, calculated at the GGA level are in good agreement with results from hybrid B3LYP and HSE06, even though, as is well known, GGA is unreliable for electronic properties such as band gaps.

Addition of the co-dopant nitrogen to Li-doped diamond reduces defect cluster-formation energies and stabilises the presence of substitutional rather than interstitial lithium, which we rationalise in terms of the strain present in the different defective structures. Key to

this is the reduction in strain due to the absence in the co-doped material with substitutional Li of long nearest-neighbour N-C distances of around 2.0 Å. These are present in N-doped diamond due to the repulsion between the unpaired electron in a carbon dangling bond and the lone pair of electrons on nitrogen. This lone pair now participates in the Li-N bond which is much closer in length to the C-C bond length in undoped diamond. In all the examples we have studied, strain effects are highly localised within a few atomic spacings of the clusters.

It is interesting that the atom-projected densities of states of the Li-, N- and Li_CN_4-doped diamond show that the chief contributions to the defect states are not from orbitals on the dopant atoms themselves but from states associated with the neighbouring carbon atoms. We conclude that only the 1:4 cluster, Li_CN_4, with substitutional Li, is likely to behave as a shallow donor, consistent with the suggestion of Moussa *et al*. [38]. A detailed thermodynamic analysis shows that under typical preparative conditions, different clusters Li_CN_x (x = 1-4) will be present. We propose a non-molecular synthetic route for the preparation of the Li_CN_4 doped material via prior generation of the N_4V centre at temperatures at which lithium atoms are mobile and isolated vacancies and Li_CN_4 clusters are not.

The calculations suggest that the Li_CN_4 cluster is, at least, a promising potential candidate for producing n-type diamond. We hope our results will prompt related experimental work. Our future computational work will concentrate on how to assist such experiments in the interpretation of spectroscopic data to distinguish between the different clusters present in order to optimise the concentrations of the Li_CN_4 defect cluster.

Acknowledgements

The authors are grateful to the Public Service Department, Government of Malaysia, EPSRC grant EP/K030302/1 for financial support and Ben Truscott for his help with the software. S.C. gratefully acknowledges the Becas Chile program (CONICYT PAI/INDUSTRIA 74150058) for a postdoctoral grant at the University of Bristol, and FONDECYT Grant 11171063. This work was carried out using the computational facilities of the Advanced Computing Research Centre, University of Bristol http://www.bris.ac.uk/acrc. The raw data for these calculations can be found on the University of Bristol data repository with d.o.i.{to be added at proofs stage}.

References

[1] P.W. May, Diamond thin films: a 21st-century material, Philos. Trans. R. Soc. London, Ser. A 358 (2000) 473-495.

[2] P. May, W. Ludlow, M. Hannaway, P. Heard, J. Smith, K. Rosser, Raman and conductivity studies of boron-doped microcrystalline diamond, facetted nanocrystalline diamond and cauliflower diamond films, Diamond Relat. Mater. 17 (2008) 105-117.

[3] T. Watanabe, S. Yoshioka, T. Yamamoto, H. Sepehri-Amin, T. Ohkubo, S. Matsumura, Y. Einaga, The local structure in heavily boron-doped diamond and the effect this has on its electrochemical properties, Carbon 137 (2018) 333-342.

[4] J. Wang, Z. He, X. Tan, T. Wang, L. Liu, X. He, X.D. Liu, L. Zhang, K. Du, High-performance 2.6 V aqueous symmetric supercapacitor based on porous boron doped diamond via regrowth of diamond nanoparticles, Carbon 160 (2020) 71-79.

[5] Z.J. Ayres, J.C. Newland, M.E. Newton, S. Mandal, O.A. Williams, J.V. Macpherson, Impact of chemical vapour deposition plasma inhomogeneity on the spatial variation of sp^2 carbon in boron doped diamond electrodes, Carbon 121 (2017) 434-442.

[6] R. Kalish, Doping of diamond, Carbon 37 (1999) 781-785.

[7] M.N. Ashfold, J.P. Goss, B.L. Green, P.W. May, M.E. Newton, C.V. Peaker, Nitrogen in Diamond, Chem. Rev. 120 (2020) 5745-5794.

[8] Z. Liang, H. Kanda, X. Jia, H. Ma, P. Zhu, Q.-F. Guan, C. Zang, Synthesis of diamond with high nitrogen concentration from powder catalyst-C-additive NaN_3 by HPHT, Carbon 44 (2006) 913-917.

[9] V. Baranauskas, B. Li, A. Peterlevitz, M. Tosin, S. Durrant, Nitrogen-doped diamond films, J. Appl. Phys. 85 (1999) 7455-7458.

[10] W. Müller-Sebert, E. Wörner, F. Fuchs, C. Wild, P. Koidl, Nitrogen induced increase of growth rate in chemical vapor deposition of diamond, Appl. Phys. Lett. 68 (1996) 759-760.

[11] R. Farrer, On the substitutional nitrogen donor in diamond, Solid State Commun. 7 (1969) 685-688.

[12] R. Kalish, C. Uzan-Saguy, B. Philosoph, V. Richter, J. Lagrange, E. Gheeraert, A. Deneuville, A. Collins, Nitrogen doping of diamond by ion implantation, Diamond Relat. Mater. 6 (1997) 516-520.

[13] A. Lazea, V. Mortet, J. D'Haen, P. Geithner, J. Ristein, M. D'Olieslaeger, K. Haenen, Growth of polycrystalline phosphorous-doped CVD diamond layers, Chem. Phys. Lett. 454 (2008) 310-313.

[14] S. Kajihara, A. Antonelli, J. Bernholc, R. Car, Nitrogen and potential n-type dopants in diamond, Phys. Rev. Lett. 66 (1991) 2010.

[15] G. Popovici, M. Prelas, T. Sung, S. Khasawinah, A. Melnikov, V. Varichenko, A. Zaitsev, A. Denisenko, W. Fahrner, Properties of diffused diamond films with n-type conductivity, Diamond Relat. Mater. 4 (1995) 877-881.

[16] J. Goss, P. Briddon, Theoretical study of Li and Na as n-type dopants for diamond, Phys. Rev. B 75 (2007) 075202.

[17] A. Mainwood, Theoretical modelling of dopants in diamond, J. Mater. Sci: Mater. Electron. 17 (2006) 453-458.

[18] E. Lombardi, A. Mainwood, Li and Na in diamond: A comparison of DFT models, Physica B 401 (2007) 57-61.

[19] S. Prawer, C. Uzan-Saguy, G. Braunstein, R. Kalish, Can n-type doping of diamond be achieved by Li or Na ion implantation?, Appl. Phys. Lett. 63 (1993) 2502-2504.

[20] R. Zeisel, C. Nebel, M. Stutzmann, H. Sternschulte, M. Schreck, B. Stritzker, Photoconductivity study of Li doped homoepitaxially grown CVD diamond, Phys. Status Solidi A 181 (2000) 45-50.

[21] M. Restle, K. Bharuth-Ram, H. Quintel, C. Ronning, H. Hofsäss, S. Jahn, ISOLDE-Collaboration, U. Wahl, Lattice sites of ion implanted Li in diamond, Appl. Phys. Lett. 66 (1995) 2733-2735.

[22] J.P. Goss, R.J. Eyre, P.R. Briddon, Theoretical models for doping diamond for semiconductor applications, Phys. Status Solidi B 245 (2008) 1679-1700.

[23] S. Halliwell, P. May, N. Fox, M. Othman, Investigations of the co-doping of boron and lithium into CVD diamond thin films, Diamond Relat. Mater. 76 (2017) 115-122.

[24] E. Lombardi, A. Mainwood, K. Osuch, Ab initio study of lithium and sodium in diamond, Phys. Rev. B 76 (2007) 155203.

[25] E. Lombardi, A. Mainwood, A first principles study of lithium, sodium and aluminum in diamond, Diamond Relat. Mater. 17 (2008) 1349-1352.

[26] J. Goss, B. Coomer, R. Jones, C. Fall, P. Briddon, S. Öberg, Extended defects in diamond: the interstitial platelet, Phys. Rev. B 67 (2003) 165208.

[27] J. Goss, P. Briddon, R. Jones, S. Sque, Donor and acceptor states in diamond, Diamond Relat. Mater. 13 (2004) 684-690.

[28] K.M. O'Donnell, M.T. Edmonds, J. Ristein, A. Tadich, L. Thomsen, Q.H. Wu, C.I. Pakes, L. Ley, Diamond Surfaces with Air-Stable Negative Electron Affinity and Giant Electron Yield Enhancement, Adv. Funct. Mater. 23 (2013) 5608-5614.

[29] K.M. O'Donnell, T.L. Martin, N.L. Allan, Light metals on oxygen-terminated diamond (100): structure and electronic properties, Chem. Mater. 27 (2015) 1306-1315.

[30] K. O'Donnell, T. Martin, N. Fox, D. Cherns, Ab initio investigation of lithium on the diamond C (100) surface, Phys. Rev. B 82 (2010) 115303.

[31] K.M. O'Donnell, T.L. Martin, N.A. Fox, D. Cherns, The Li-adsorbed C (100)-(1x1): O diamond surface, MRS Proceedings 1282 (2011) Mrsf10-1282-a1205-1204.

[32] K.M. O'Donnell, M.T. Edmonds, A. Tadich, L. Thomsen, A. Stacey, A. Schenk, C.I. Pakes, L. Ley, Extremely high negative electron affinity of diamond via magnesium adsorption, Phys. Rev. B 92 (2015) 035303.

[33] A.K. Tiwari, J. Goss, P. Briddon, N. Wright, A. Horsfall, M. Rayson, Bromine functionalisation of diamond: An ab initio study, Phys. Status Solidi A 209 (2012) 1703-1708.

[34] A.K. Tiwari, J. Goss, P. Briddon, N.G. Wright, A.B. Horsfall, R. Jones, H. Pinto, M. Rayson, Calculated electron affinity and stability of halogen-terminated diamond, Phys. Rev. B 84 (2011) 245305.

[35] A.K. Tiwari, J. Goss, P. Briddon, N. Wright, A. Horsfall, M. Rayson, Effect of different surface coverages of transition metals on the electronic and structural properties of diamond, Phys. Status Solidi A 209 (2012) 1697-1702.

[36] A.K. Tiwari, J. Goss, P. Briddon, N.G. Wright, A.B. Horsfall, M. Rayson, Electronic and structural properties of diamond (001) surfaces terminated by selected transition metals, Phys. Rev. B 86 (2012) 155301.

[37] A.K. Tiwari, J. Goss, P. Briddon, N. Wright, A. Horsfall, R. Jones, H. Pinto, M. Rayson, Thermodynamic stability and electronic properties of F-and Cl-terminated diamond, Phys. Status Solidi A 209 (2012) 1709-1714.

[38] W. Paxton, M. Howell, W. Kang, J. Davidson, Influence of hydrogen on the thermionic electron emission from nitrogen-incorporated polycrystalline diamond films, J. Vac. Sci. Technol. B 30 (2012) 021202.

[39] W. Paxton, A. Steigerwald, M. Howell, N. Tolk, W. Kang, J. Davidson, The effect of hydrogen desorption kinetics on thermionic emission from polycrystalline chemical vapor deposited diamond, Appl. Phys. Lett. 101 (2012) 243509.

[40] T.Y. Sun, F.A. Koeck, R.J. Nemanich, Thermionic and photon-enhanced emission from CVD diamond: influence of nanostructure, doping, and substrate, Adv. Sci. and Tech. 95 (2014) 1-10.

[41] K. Czelej, P. Śpiewak, K.J. Kurzydłowski, Electronic structure of substitutionally doped diamond: Spin-polarized, hybrid density functional theory analysis, Diamond Relat. Mater. 75 (2017) 146-151.

[42] A. Croot, M.Z. Othman, S. Conejeros, N.A. Fox, N.L. Allan, A theoretical study of substitutional boron–nitrogen clusters in diamond, J. Phys.: Condens. Matter 30 (2018) 425501.

[43] S. Salustro, F. Colasuonno, A.M. Ferrari, M. D'Amore, W.C. Mackrodt, R. Dovesi, Substitutional boron and nitrogen pairs in diamond. A quantum mechanical vibrational analysis, Carbon 146 (2019) 709-716.

[44] X. Hu, R. Li, H. Shen, Y. Dai, X. He, Electrical and structural properties of boron and phosphorus co-doped diamond films, Carbon 42 (2004) 1501-1506.

[45] M.Z. Othman, P.W. May, N.A. Fox, In-situ Incorporation of Lithium and Nitrogen into CVD Diamond Thin Films, MRS Proceedings 1511 (2013) mrsf12-1511-ee1505-1505.

[46] M.Z. Othman, P.W. May, N.A. Fox, P.J. Heard, Incorporation of lithium and nitrogen into CVD diamond thin films, Diamond Relat. Mater. 44 (2014) 1-7.

[47] J.E. Moussa, N. Marom, N. Sai, J.R. Chelikowsky, Theoretical Design of a Shallow Donor in Diamond by Lithium-Nitrogen Codoping, Phys. Rev. Lett. 108 (2012) 226404.

[48] G. Popovici, M. Prelas, Prospective n-type impurities and methods of diamond doping, Diamond Relat. Mater. 4 (1995) 1305-1310.

[49] M. Taylor, G. Barrera, N.L. Allan, T. Barron, W. Mackrodt, Free energy of formation of defects in polar solids, Faraday Discuss. 106 (1997) 377-387.

[50] S.J. Clark, M.D. Segall, C.J. Pickard, P.J. Hasnip, M.I. Probert, K. Refson, M.C. Payne, First principles methods using CASTEP, Zeitschrift für Kristallographie-Crystalline Materials 220 (2005) 567-570.

[51] M. Segall, P.J. Lindan, M.a. Probert, C. Pickard, P. Hasnip, S. Clark, M. Payne, First-principles simulation: ideas, illustrations and the CASTEP code, J. Phys.: Condens. Matter 14 (2002) 2717.

[52] J.P. Perdew, K. Burke, M. Ernzerhof, Generalized Gradient Approximation Made Simple, Phys. Rev. Lett. 77 (1996) 3865-3868.

[53] R. Nicholls, A. Morris, C. Pickard, J. Yates, OptaDOS-a new tool for EELS calculations, J. Phys.: Conf. Ser. 371 (2012) 012062.

[54] A.D. Becke, Becke's three parameter hybrid method using the LYP correlation functional, J. Chem. Phys. 98 (1993) 5648-5652.

[55] A.V. Krukau, O.A. Vydrov, A.F. Izmaylov, G.E. Scuseria, Influence of the exchange screening parameter on the performance of screened hybrid functionals, J. Chem. Phys. 125 (2006) 224106.

[56] G. Di Palma, B. Kirtman, F.S. Gentile, A. Platonenko, A.M. Ferrari, R. Dovesi, The VN2 negatively charged defect in diamond. A quantum mechanical investigation of the EPR response, Carbon 159 (2020) 443-450.

[57] R. Dovesi, F.S. Gentile, A.M. Ferrari, F. Pascale, S. Salustro, P. D'arco, On the Models for the Investigation of Charged Defects in Solids: The Case of the VN–Defect in Diamond, J. Phys. Chem. A 123 (2019) 4806-4815.

[58] F. Pascale, S. Salustro, A.M. Ferrari, M. Rérat, P. D'arco, R. Dovesi, The Infrared spectrum of very large (periodic) systems: global versus fragment strategies-the case of three defects in diamond, Theor. Chem. Acc. 137 (2018) 170.

[59] F.S. Gentile, S. Salustro, G. Di Palma, M. Causá, P. D'arco, R. Dovesi, Hydrogen, boron and nitrogen atoms in diamond: a quantum mechanical vibrational analysis, Theor. Chem. Acc. 137 (2018) 154.

[60] A.M. Ferrari, S. Salustro, F.S. Gentile, W.C. Mackrodt, R. Dovesi, Substitutional nitrogen atom in diamond. A quantum mechanical investigation of the electronic and spectroscopic properties, Carbon 134 (2018) 354-365.

[61] S. Salustro, F. Pascale, W.C. Mackrodt, C. Ravoux, A. Erba, R. Dovesi, Interstitial nitrogen atoms in diamond. A quantum mechanical investigation of its electronic and vibrational properties, Phys. Chem. Chem. Phys. 20 (2018) 16615-16624.

[62] S. Salustro, F.S. Gentile, A. Erba, P. Carbonniére, K.E. El-Kelany, R. Dovesi, The characterization of the VN_xH_y defects in diamond through the infrared vibrational spectrum. A quantum mechanical investigation, Carbon 132 (2018) 210-219.

[63] F.S. Gentile, S. Salustro, J.K. Desmarais, A.M. Ferrari, P. D'Arco, R. Dovesi, Vibrational spectroscopy of hydrogens in diamond: a quantum mechanical treatment, Phys. Chem. Chem. Phys. 20 (2018) 11930-11940.

[64] S. Salustro, F. Gentile, P. d'Arco, B. Civalleri, M. Rérat, R. Dovesi, Hydrogen atoms in the diamond vacancy defect. A quantum mechanical vibrational analysis, Carbon 129 (2018) 349-356.

[65] R. Dovesi, A. Erba, R. Orlando, C.M. Zicovich-Wilson, B. Civalleri, L. Maschio, M. Rérat, S. Casassa, J. Baima, S. Salustro, Quantum-mechanical condensed matter simulations with CRYSTAL, Wiley Interdiscip. Rev. Comp. Mol. Sci. (2018) e1360.

[66] See http://www.crystal.unito.it for details on the CRYSTAL code Gaussian basis sets computational schemes, etc.

[67] R. Dovesi, V.R. Saunders, R. Roetti, R. Orlando, C.M. Zicovich-Wilson, F. Pascale, B. Civalleri, K. Doll, N.M. Harrison, I.J. Bush, P. D'Arco, M. Llunell, M. Causà, Y. Noël, L.

Maschio, A. Erba, M. Rerat and S. Casassa, CRYSTAL17 User's Manual (University of Torino, Torino, 2017).

[68] M. Catti, A. Pavese, R. Dovesi, V. Saunders, Static lattice and electron properties of $MgCO_3$ (magnesite) calculated by ab initio periodic Hartree-Fock methods, Phys. Rev. B 47 (1993) 9189.

[69] M.F. Peintinger, D.V. Oliveira, T. Bredow, Consistent Gaussian basis sets of triple-zeta valence with polarization quality for solid-state calculations, J. Comput. Chem. 34 (2013) 451-459.

[70] R. Dovesi, R. Orlando, B. Civalleri, C. Roetti, V.R. Saunders, C.M. Zicovich-Wilson, CRYSTAL: a computational tool for the ab initio study of the electronic properties of crystals, Z. Kristallogr. 220 (2005) 571-573.

[71] C.G. Van de Walle, J. Neugebauer, First-principles calculations for defects and impurities: Applications to III-nitrides, J. Appl. Phys. 95 (2004) 3851-3879.

[72] H. Sternschulte, M. Schreck, B. Stritzker, A. Bergmaier, G. Dollinger, Lithium addition during CVD diamond growth: influence on the optical emission of the plasma and properties of the films, Diamond Relat. Mater. 9 (2000) 1046-1050.

[73] B.S. Truscott, M.W. Kelly, K.J. Potter, M. Johnson, M.N. Ashfold, Y.A. Mankelevich, Microwave Plasma-Activated Chemical Vapor Deposition of Nitrogen-Doped Diamond. I. N_2/H_2 and NH_3/H_2 Plasmas, J. Phys. Chem. A 119 (2015) 12962-12976.

[74] B.S. Truscott, M.W. Kelly, K.J. Potter, M.N. Ashfold, Y.A. Mankelevich, Microwave plasma-activated chemical vapor deposition of nitrogen-doped diamond. II: $CH_4/N_2/H_2$ plasmas, J. Phys. Chem. A 120 (2016) 8537-8549.

[75] R.W.G. Wyckoff, R.W. Wyckoff, Crystal structures, Interscience New York, 1960.

[76] J.E. Field, The properties of natural and synthetic diamond, Academic Press, London, 1992.

[77] J.P. Perdew, Density functional theory and the band gap problem, Int. J. Quantum Chem. 28 (1985) 497-523.

[78] C.G. Van de Walle, A. Janotti, Advances in electronic structure methods for defects and impurities in solids, Phys. Status Solidi B 248 (2011) 19-27.

[79] J. Paier, M. Marsman, K. Hummer, G. Kresse, I.C. Gerber, J.G. Ángyán, Screened hybrid density functionals applied to solids, J. Chem. Phys. 124 (2006) 154709.

[80] L. Allers, A. Mainwood, Surface vacancies in CVD diamond, Diamond Relat. Mater. 7 (1998) 261-265.

[81] A. Neves, M.H. Nazaré, Properties, growth and applications of diamond, IET, 2001.

[82] Y. Bar-Yam, T. Moustakas, Defect-induced stabilization of diamond films, Nature 342 (1989) 786-787.

[83] W. Banholzer, Understanding the mechanism of CVD diamond, Surf. Coat. Technol. 53 (1992) 1-12.

[84] S. Dannefaer, W. Zhu, T. Bretagnon, D. Kerr, Vacancies in polycrystalline diamond films Phys. Rev. B, 53 (1996) 1979.

[85] M. Grujicic, S. Lai, Atomistic simulation of chemical vapor deposition of (111)-oriented diamond film using a kinetic Monte Carlo method, J. Mater. Sci. 34 (1999) 7-20.

[86] M. Grujicic, S. Lai, Multi-length scale modeling of CVD of diamond Part IA combined reactor-scale/atomic-scale analysis, J. Mater. Sci. 35 (2000) 5359-5369.

[87] M. Grujicic, S. Lai, Multi-length scale modeling of CVD of diamond Part II A combined atomic-scale/grain-scale analysis, J. Mater. Sci. 35 (2000) 5371-5381.

[88] E. Weiss, G. Hencken, Über metall-alkyl-verbindungen: XII. verfeiner ung der kristallstruktur des methyllithiums, J. Organomet. Chem. 21 (1970) 265-268.

[89] R.E. Dinnebier, U. Behrens, F. Olbrich, Lewis base-free phenyllithium: Determination of the solid-state structure by synchrotron powder diffraction, J. Am. Chem. Soc. 120 (1998) 1430-1433.

[90] E. Gheeraert, S. Koizumi, T. Teraji, H. Kanda, Electronic transitions of electrons bound to phosphorus donors in diamond, Solid State Commun. 113 (2000) 577-580.

[91] J.P Goss, M.J. Shaw, P.R. Briddon, Marker-method calculations for electrical levels using Gaussian-orbital basis sets, in: Theory of defects in semiconductors, Springer, 2007, pp. 69-94.

[92] A. Zelferino, S. Salustro, J. Baima, V. Lacivita, R. Orlando, R. Dovesi, The electronic states of the neutral vacancy in diamond: a quantum mechanical approach, Theor. Chem. Acc. 135 (2016) 74.

[93] G. Sansone, S. Salustro, Y. Noël, L. Maschio, W.C. Mackrodt, R. Dovesi, Looking for sp^2 carbon atoms in diamond: a quantum mechanical study of interacting vacancies, Theor. Chem. Acc. 137 (2018) 29.

[94] M. Capelli, A. Heffernan, T. Ohshima, H. Abe, J. Jeske, A. Hope, A. Greentree, P. Reineck, B. Gibson, Increased nitrogen-vacancy centre creation yield in diamond through electron beam irradiation at high temperature, Carbon 143 (2019) 714-719.

[95] J. Forneris, S.D. Tchernij, A. Tengattini, E. Enrico, V. Grilj, N. Skukan, G. Amato, L. Boarino, M. Jakšić, P. Olivero, Electrical control of deep NV centers in diamond by means of sub-superficial graphitic micro-electrodes, Carbon 113 (2017) 76-86.

[96] J. Baker, A new proposal for the structure of platelets in diamond, Diamond Relat. Mater. 7 (1998) 1282-1290.

[97] T. Miyazaki, H. Okushi, A theoretical study of a sulfur impurity in diamond, Diamond Relat. Mater. 10 (2001) 449-452.

[98] V.A. Nadolinny, O.P. Yurjeva, N.P. Pokhilenko, EPR and luminescence data on the nitrogen aggregation in diamonds from Snap Lake dyke system, Lithos 112 (2009) 865-869.

[99] A. Yelisseyev, G. Meng, V. Afanasyev, N. Pokhilenko, V. Pustovarov, A. Isakova, Z. Lin, H. Lin, Optical properties of impact diamonds from the Popigai astrobleme, Diamond Relat. Mater. 37 (2013) 8-16.

[100] D. Palmer, in Properties and Growth of Diamond, Ed. G. Davies in, IEE/INSPEC, London, 1994.

[101] R. Mildren and J. Rabeau, Optical engineering of diamond, Eds. Wiley-VCH Verlag GmbH & Co. KGaA: Weinheim, Germany, 2013.

FIGURE CAPTIONS

Fig 1. Two LiN_4 clusters studied: (a) substitutional Li (Li_CN_4) and (b) interstitial (Li_iN_4) with the interstitial atom at the T_d site. C atoms are yellow, N atoms are blue and Li atoms are green.

Fig. 2. Hybrid (HSE06) DOS of (a) pure diamond, (b) carbon vacancy and (c) N-doped diamond (S = 1/2) with substitutional nitrogen for the 64-atom supercell. (d) Hybrid (HSE06) DOS of Li_i-doped diamond (interstitial, T_d site) for the 65-atom supercell (S = 1/2). (e) Hybrid (HSE06) DOS of Li-doped diamond (substitutional) from the 64-atom supercell. In (c), (d), (e) and (f) both the total DOS and the projected DOS for the dopant atom are shown. In this and all subsequent figures the energy of the highest occupied state is arbitrarily set to zero and indicated by the vertical dashed lines. The upper and lower frames show the DOS for spin-up and spin-down electrons respectively.

Fig. 3. Bond lengths (in italics) and Mulliken net charges (in *e*) in Li_CN_4. The labels *a*, *b* and *c* denote symmetrically equivalent carbon atoms.

Fig. 4. (a) and (b): Hybrid (HSE06) DOS for Li_CN_4 co-doped diamond (substitutional) for (a) 64- and (b) 144-atom supercells, $C_{59}Li_CN_4$.and $C_{143}Li_CN_4$, respectively. The total DOS and the projected DOS for the dopant atoms are shown. The highest occupied states are arbitrarily assigned a value of zero and are indicated by vertical dashed lines. Note these are diamagnetic conducting solutions.

Fig. 5. Unrelaxed geometries of two further possible arrangements of Li_CN_4 clusters (cluster 2 and cluster 3). Cluster 1 is shown in Figure 1a. C atoms are yellow, N atoms blue and Li green.

Fig. 6. B3LYP energies of possible experimental pathways for the synthesis of Li_CN_x co-doped diamond. C atoms are yellow, N atoms are blue and Li atoms are green.